

Special Issue: "Data Science, Geoinformatics and Systems Analysis in Geosciences"

CURIE POINT DEPTHS OF THE AMUR TECTONIC PLATE

A. N. Didenko^{1,2}, M. Yu. Nosyrev², G. Z. Gilmanova²

Abstract: Based on the analysis of the anomaly magnetic field for the Amur Plate and adjacent territories, a Curie Point Depth (CPD) map has been constructed, which we identify with the isotherm 578°C — the temperature of the Curie point of magnetite. Within the Amur plate, the CPD values range from 13.4 to 38.0 km. Three large areas are clearly visible on the map: 1) NE-trending zone with CPD values of 25–20 km — Yellow Sea-Korean Peninsula-Sea of Japan; 2) ENE-trending central zone with CPD values of 30–38 km. Large depth values are due to the presence of the late Paleozoic and Mesozoic sedimentary basins of Erlyan, Songliao and Sredneamursky; 3) ENE-trending central zone with CPD values of 30–38 km. Large depth values are due to the presence of the late Paleozoic and Mesozoic sedimentary basins of Erlyan, Songliao and Sredneamursky. The fourth area of decrease in CPD values spatially coincides with volcanic structures of Pliocene-Pleistocene age in the area of the Toko Stanovik. Comparison of the generated CPD map with the Amur plate boundaries determined mainly from seismic data shows that the surface boundaries of the plate coincide mainly with the zones of the largest gradients of the 578°C isotherm distribution in depth.

Keywords: Amur plate, anomaly magnetic field, spectral analysis, Curie point depth.

Citation: Didenko, A. N., M. Yu. Nosyrev, and G. Z. Gilmanova (2025), Curie Point Depths of the Amur Tectonic Plate, *Russian Journal of Earth Sciences*, 25, ES2005, EDN: NUVKQI, https://doi.org/10.2205/2025ES000964

1. Introduction

The structural study of the upper shell of the solid Earth based on spectral analysis of magnetic anomalies is one of the components of deep investigations using a multidisciplinary approach. And while in the vast majority of cases the magnetized layer on the continents is located within the earth's crust, in the case of the oceanic lithosphere, secondary magnetic rocks (serpentinized ultrabasites) belong to the upper mantle according to petrological criteria. The main task here is to determine the depth to the bottom of the magnetized layer or, as it is often called, the Curie Point Depth (CPD). The presence of this boundary is due to an increase in temperature with depth and a transition of accessory magnetic minerals found in rocks from a ferrimagnetic state to a paramagnetic one. For continental regions, this is the Curie temperature for magnetite which is the main carrier of magnetism in the continental lithosphere.

Within continental areas, the distribution of surface heat flow and deep thermal structures may differ due to the long-term evolution of the latter and thermal disturbances at late stages through filtration and rise of fluids to the surface. In continental lithosphere, delays may be observed between changes in temperature of the underlying asthenospheric and surface heat flow measurements. The heat generated by the radioactive decay of K, U, and Th isotopes also contributes to the total surface heat flow of the continents. Therefore, the CPD estimation and interpretation is important both in connection with the study of deep mantle heat flow, and from the point of view of structural, tectonic and geodynamic reconstructions.

RESEARCH ARTICLE

Received: 15 November 2024 Accepted: 15 April 2025 Published: 23 May 2025



Copyright: © 2025. The Authors. This article is an open access article distributed under the terms and conditions of the Creative Commons Attribution (CC BY) license (https://creativecommons.org/licenses/by/4.0).

¹Geological Institute RAS, Moscow, Russia

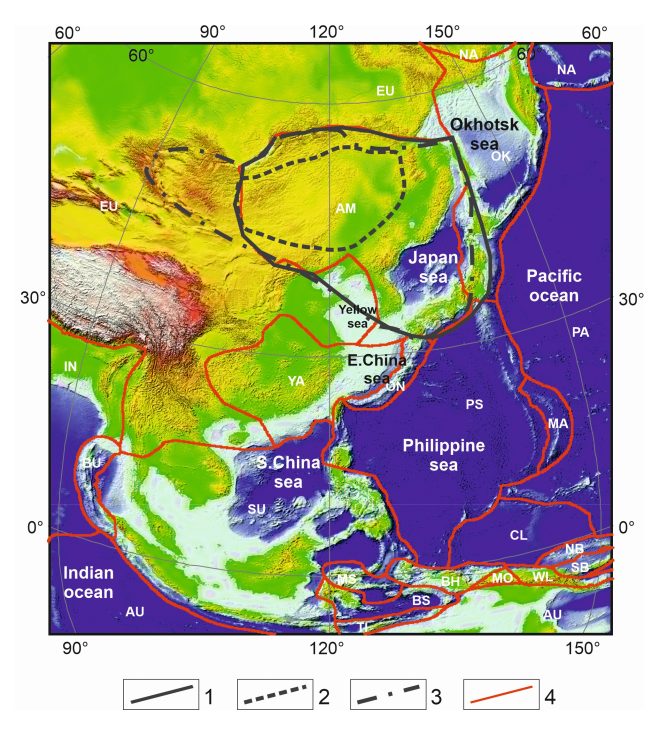
²Institute of Tectonics & Geophysics FEB RAS, Khabarovsk, Russia

^{*} Correspondence to: Didenko Alexei N., alexei_didenko@mail.ru

Large tectonic units of the southern Far East are characterized by CPD values only within limited areas [*Didenko et al.*, 2017; *Gao et al.*, 2015; *Wang et al.*, 2018; *Xiong et al.*, 2016], which makes it difficult to obtain a complete picture of the deep structure of the eastern Central Asian fold belt and its junction with the Pacific belt. To fill this gap, we chose the Amur plate (Figure 1), which is one of the main tectonic megastructures in the southeast of the Eurasian continent at the Mesozoic-Cenozoic geodynamic stage, as an object of CPD estimations. The following tasks were defined for the study: 1) estimation of the depth to the bottom of magnetic sources using the centroid method based on spectral analysis of magnetic anomalies [*Tanaka et al.*, 1999] of CPD for window squares of 200×200 km covering the entire Amur plate and adjacent territories; and 2) construction of a CPD model of the Amur plate and adjacent territories using the ArcGis geospatial platform [*ArcGIS...*, 2011].



(a) Amur plate is highlighted by white hatching. Orthographic projection, central meridian is 120°.



(b) 1–4 — boundaries of the Amur lithospheric plate after: 1 — [Yarmolyuk et al., 2019], 2 — [Imaev et al., 2003], 3 — [Petit et al., 2004], 4 — [Argus et al., 2011]. The plates are indicated by abbreviations: AM — Amur, AU — Australian, BH — Birds Head, BS — Banda Sea, BU — Burma, CL — Caroline, EU — Eurasia, IN — India, MA — Mariana, MO — Maoke, MS — Molucca Sea, NA — North America, NB — North Bismarck, OK — Okhotsk, ON — Okinawa, PA — Pacific, PS — Philippine Sea, SB — South Bismarck, SA — Sunda, TI — Timor, WL — Woodlark (Woodlark), YA — Yangtze. Orthographic projection, central meridian is 120°.

Figure 1. Position of the Amur plate: a on the world map and b in the system of lithospheric tectonic plates of Southeast Asia after [*Argus et al.*, 2011] with amendments and additions.

It should be mentioned that the CPD value was calculated for the entire Earth, except for the polar regions [*Li et al.*, 2017], using the fractal method based on the analysis of the EMAG2 Earth Magnetic Anomaly Model [*Maus et al.*, 2009]. Firstly, in our study, we used the latest EMAG2 version 3 [*Meyer et al.*, 2017] grid, and secondly, CPD estimations were performed using the classical centroid method [*Tanaka et al.*, 1999].

2. Boundaries of the Amur lithospheric plate

Continental and subcontinental lithospheric plates are complex in geological structure and composition, which is, to a large extent, characteristic of plate boundaries represented as extended banded zones of hummocking and fragmentation, the identification of which is often controversial [*Deep Structure...*, 2010]. This fully applies to the Amur lithospheric plate.

Since the identification of the Amur lithospheric plate as a self-dependent geodynamic unit [Yarmolyuk et al., 2019] its boundaries have been the subject of debate. There are at least 10 variants of the Amur plate boundaries; for more details see [Ashurkov et al., 2011; Li et al., 2019]. Figure 1b, in addition to the first model of plate boundaries after [Yarmolyuk et al., 2019], shows three more models. The first two are models of extreme values in terms of area covered: the minimum area model of [Imaev et al., 2003] and the maximum area model of [Petit et al., 2004]. And the third is the Global Plate Model [Argus et al., 2011], which is most often used in present-day geodynamic reconstructions and is in good agreement with the model developed by [Yarmolyuk et al., 2019], with the exception of the southern part of Sakhalin, Hokkaido, the northern part of Honshu Island and the Yellow Sea. The most recent model of the Amur plate boundary is used in this study.

3. The data used and methodology of estimations

The anomalous magnetic field of the Amur plate area (Figure 2) is heterogeneous and reflects the large tectonic units of the region according to the magnetic properties of the rocks that compose them. The field strength varies from -637 to +1366 nT at an amplitude of about 700 nT, without taking into account local positive magnetic anomalies in iron ore deposits. Sedimentary terranes of orogenic belts, Mesozoic-Cenozoic superimposed troughs and depressions filled with non-magnetic sediments are distinguished by a reduced and weakly differentiated magnetic field. The marginal parts of cratons and ancient blocks in the Central Asian belt are characterized by an alternating magnetic field, where positive magnetic anomalies are associated with both ancient metamorphosed basic and ultrabasic igneous rocks, and late basic intrusions. Northeast-oriented anomalous zones are dominant in the magnetic field, with two main strike azimuths of approximately 30 and 60 degrees. Zones of positive magnetic anomalies of this orientation are hundreds to thousands of kilometers long with a width of 100-200 km. The calculations were carried out using the centroid method under the assumption of a random distribution of magnetic sources [Tanaka et al., 1999] with the determination of their top and bottom. This method was chosen, first of all, for the absence of any requirements for preliminary knowledge of the magnetization of the medium.

At the initial stage, taking into account the large extent of the study area from north to south, the magnetic field was transformed to the pole. Then, considering the range of CPD values in the interval between 13 and 48 km based on the data from previous studies in discrete regions of Southeast Asia [Didenko et al., 2017; Gao et al., 2015; Wang et al., 2018; Xiong et al., 2016], the entire study area was divided into square windows of 200×200 km, for which depths to the bottom of the magnetized layer were calculated. The window step in longitude was 100 km (i.e. with 50% overlap), in latitude — 200 km. The calculation results were related to the window center. As a result, the calculations were performed in 940 windows, with the network of window central points of 100×200 km.

The subsequent steps for each sheet included the same operations.

- 1. Calculation of the average circular energy spectrum for each sheet based on the implementation of the fast Fourier transform.
- 2. Calculation of spectra to estimate the depths to the centroid and top of the magnetic body after [*Tanaka et al.*, 1999] using the following formulas:

$$\ln\left[\frac{P^{1/2}}{|S|}\right] = \ln A - 2\pi |S| Z_0$$

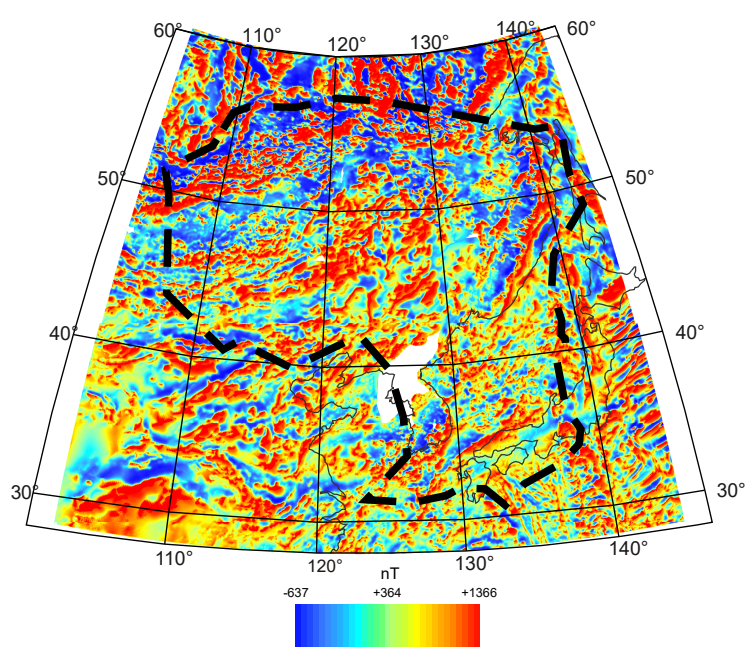


Figure 2. Maps of the anomalous magnetic field. Observed anomalous field based on the EMAG2v3 model [*Meyer et al.*, 2017]. Amur plate boundaries are shown by a black dashed line. The Gauss-Kruger projection is used, the central meridian is 123°.

and

$$\ln P^{1/2} = \ln B - 2\pi |S| Z_t$$

where Z_0 , Z_t — centroid and top bound of the magnetic source, respectively, P — power spectrum, S — cyclic frequency, A and B — magnetization-dependent constants.

3. Since P and S are known from the previously calculated spectrum, Z_0 and Z_t are estimated, and then the depth to the bottom of the magnetic body: $Z_b = 2Z_0 - Z_t$. Since the magnetic field model [Meyer et al., 2017] is computed for an altitude of 4 km above the geoid surface, a correction is introduced in Z_b to bring it to the true depth.

Another important aspect of the calculation method is the choice of frequency intervals for determining the center (Z_0) and the upper edge of the centroid (Z_t). Based on the analysis of the above mentioned works, the interval 0–0.025 cycles/km (0–0.157 rad×km⁻¹) was chosen for calculating Z_0 , and the interval 0.042–0.075 cycles/km (0.26–0.47 rad×km⁻¹) was chosen for calculating Z_t . The calculation intervals were fixed for all spectra.

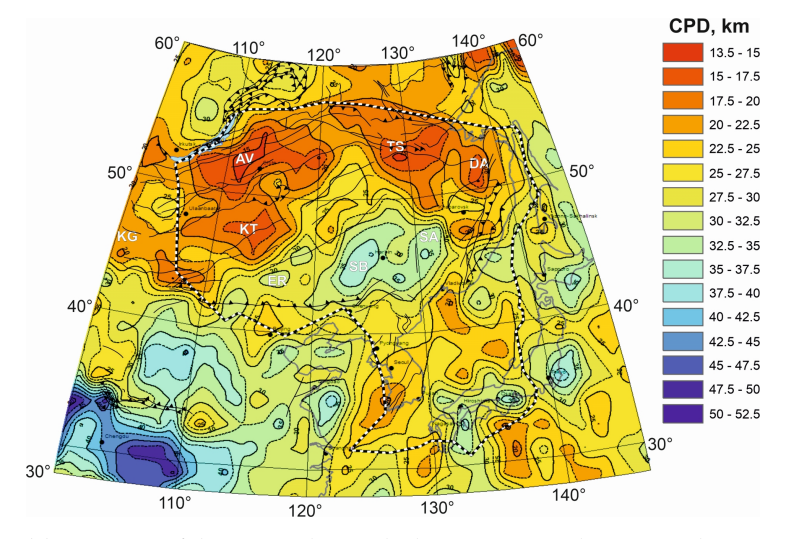
3.1. A brief introduction to the CPD map and some conclusions

Depth calculations in ArcGis, using the Natural Neighbor algorithm, culminated in CPD map construction (Figure 3a), which we identified with the 578 °C isotherm, that is, the Curie temperature for magnetite.

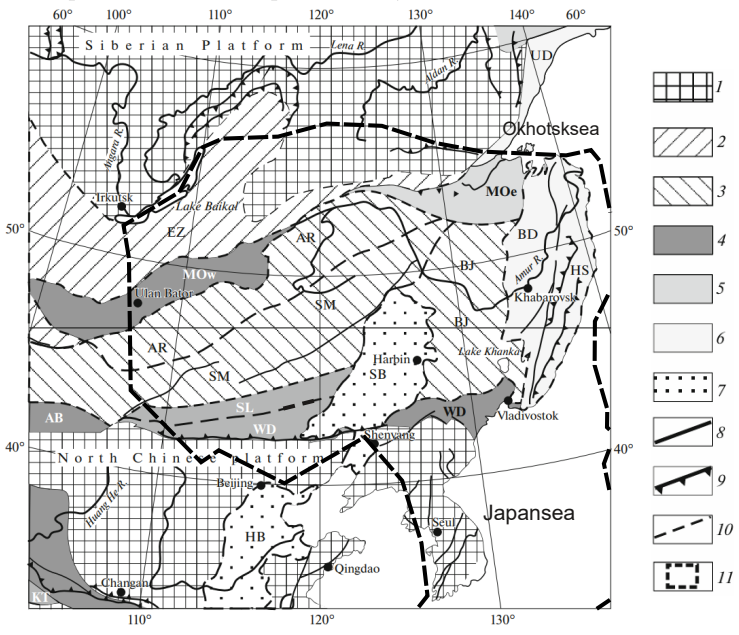
Within the Amur plate, the CPD values range from 13.4 to 38.0 km; and although the geometric mean (23.8), median (24.3), and mode (25.3) are close to the arithmetic mean (24.5 \pm 5.7), the Shapiro-Wilk test showed a significant deviation from the normal distribution (p = 0.0008, W = 0.9793) with right-sided asymmetry (0.26) and negative excess (-0.7062).

The computed map (Figure 3a) is differentiated, with three distinct domains:

NE-trending zone with CPD values of 25–20 km — Yellow Sea-Korean Peninsula-Sea of Japan (Figure 3a). The basement area of the Korean Peninsula is composed of Precambrian rocks and belongs to the North China Platform (Figure 3b), whereas the opening of the Sea of Japan began in the Middle Miocene by breaking off and rotating counterclockwise (roll-back mechanism) of the northeastern segment of the Japanese Island Arc;



(a) Map CPD of the Amur plate and adjacent areas and tectonic scheme.



(b) Map CPD of of the eastern Central Asian fold belt.

Figure 3. a. CPD map (this study). Letter designations indicate distribution areas of: 1) giant and large granitoid batholiths (AV – Angara-Vitim, DA – Dusse-Alin, KG – Khangai, KT – Khantei); 2) mantle feeder structures (TS – Toka, Verkhne-Zeya, Zeya); 3) sedimentary basins (ER -Erlian), SA – Sredneamursky, SB – Songliao). Position and type of faults are copied from (b).

b. Tectonic scheme compiled after [Didenko et al., 2016] with additions. (1) undivided Precambrian crust; (2–6) orogenic belts: (2) Caledonian, (3) Variscan (Hercynian); (4) Early Cimmerian, (5) Late Cimmerian, (6) Pacific (Yan Shan); (7) Mesozoic sedimentary basins; (8) faults, (9) thrust faults; (10) boundaries of terranes; (11) boundary of the Amur Plate. Letters show orogenic belts (terranes): (AB) Atas-Bogdo, (AR) Argun–Mamyn, (BD) Badzhal, (BJ) Bureya-Jiamusi, (EZ) Yenisei-Transbaikalia, (HS) Sikhote Alin, (KT) Kun Lun–Tsilin, (MOw) Mongol–Okhtsk (western), (MOe) Mongol–Okhotsk (eastern), (SL) Solonker, (SM) South Mongol–Khingan, (UD) Uda volcanic belt, (WD) Wundurmiao (Shara-Muren); Sedimentary basins: (HB) Hubei, (SB) Songliao.

In (a) and (b) the Gauss-Kruger projection is used, the central meridian is 123°.

• ENE-trending central zone with CPD values of 30–38 km. Large depth values are due to the presence of the late Paleozoic and Mesozoic sedimentary basins of Erlyan, Songliao and Sredneamursky (Figure 3a). The generalized tectonic diagram also clearly

- shows the northeast strike zone formed by sedimentary basins Hubei in the south and Songliao in the north (Figure 3b);
- northern zone of sublatitudinal strike with CPD values between 13.4 and 22 km. Figure 3a shows four areas of reducing the CPD. In the west and east, three areas spatially coincide with the late Paleozoic Angara-Vitim and Mesozoic Khentei and Dusse-Alin giant granitoid batholiths [Yarmolyuk et al., 2019]. The formation of gigantic masses of granitoids in these three areas is probably associated with the closure of the Mongol-Okhotsk Paleocean. This can be confirmed by the spatial coincidence of the minimum CPD depths in the northern zone (Figure 3a) with the Early Cimmerian in the west and Late Cimmerian in the east orogenic belts (Figure 3b), marking the closure of the western and eastern parts of the Mongol-Okhotsk paleoocean, respectively. In the center of the zone of reducing the CPD, in the area of the Toko-Stanovik, Yu. F. Malyshev recognized the so-called mantle feeder structures identified with a mantle plume (quoted from [Sakhno, 2008]). This is supported by numerous volcanic structures in the area of the Toko-Stanovik filled with alkaline basaltoids with an age of 0.28–7.9 Ma [Sakhno, 2008].

It can be argued that the features of drawing the CPD map of the Amur Plate (Figure 3a), performed in this work, find a completely acceptable explanation when compared with the tectonic structure of the region (Figure 3b).

Comparison of the generated CPD map with the Amur plate boundaries determined mainly from seismic data [$Argus\ et\ al.,\ 2011$] and shown in Figure 1, (shows that the surface boundaries of the plate coincide mainly with the zones of the largest gradients of the 578 °C isotherm distribution in depth.

Acknowledgments. The authors express their gratitude to the anonymous reviewer of the manuscript, most of whose comments were taken into account when preparing the final version of the work. The study was supported by the Russian Science Foundation Grant (Project No. 25-17-68001 (extended from No. 22-17-00023)). Basic funding came through the implementation of state assignments of the Geological Institute of the Russian Academy of Sciences (research topic No. FMMG-2023-0010) and the Institute of Tectonics and Geophysics, Far Eastern Branch, Russian Academy of Sciences (research topics No. 121021000095-1).

References

ArcGIS Desktop: Release 10. — Redlands, CA: ESRI, 2011.

Argus D. F., Gordon R. G., DeMets C. Geologically current motion of 56 plates relative to the no-net-rotation reference frame // Geochemistry, Geophysics, Geosystems. — 2011. — Vol. 12, no. 11. — DOI: 10.1029/2011gc003751.

Ashurkov S. V., Sankov V. A., Miroshnichenko A. I., et al. GPS geodetic constraints on the kinematics of the Amurian Plate // Russian Geology and Geophysics. — 2011. — Vol. 52, no. 2. — P. 239–249. — DOI: 10.1016/j.rgg.2010.12.017.

Deep Structure and Metallogeny of East Asia / ed. by A. N. Didenko, Y. F. Malyshev, B. G. Saksin. — Vladivostok: Dalnauka, 2010. — 332 p. — (In Russian).

Didenko A. N., Li Y.-F., Peskov A. Y., et al. Closure of the Solonker basin: Paleomagnetism of the Linxi and Xingfuzhilu formations (Inner Mongolia, China) // Russian Journal of Pacific Geology. — 2016. — Vol. 10, no. 5. — P. 317–336. — DOI: 10.1134/s181971401605002x.

Didenko A. N., Nosyrev M. Y., Shevchenko B. F., et al. Thermal structure of Sikhote Alin and adjacent areas based on spectral analysis of the anomalous magnetic field // Doklady Earth Sciences. — 2017. — Vol. 477, no. 1. — P. 1368–1372. — DOI: 10.1134/s1028334x17110198.

Gao G., Kang G., Li G., et al. Crustal magnetic anomaly and Curie surface beneath Tarim Basin, China, and its adjacent area // Canadian Journal of Earth Sciences. — 2015. — Vol. 52, no. 6. — P. 357–367. — DOI: 10.1139/cjes-2014-0204.

Imaev V. S., Imaeva L. P., Kozmin B. M. Buffer seismogenic structures between the Eurasian and Amur lithospheric plates in southern Siberia // Tikhookeanskaya Geologiya. — 2003. — Vol. 22. — P. 55–61. — (In Russian).

Li C.-F., Lu Y., Wang J. A global reference model of Curie-point depths based on EMAG2 // Scientific Reports. — 2017. — Vol. 7, no. 1. — DOI: 10.1038/srep45129.

- *Li S. H., Li C., Wang C. X.* Boundaries of the Amurian Plate identified using multiple geophysical methods // Geosciences Journal. 2019. Vol. 24, no. 1. P. 49–59. DOI: 10.1007/s12303-019-0011-1.
- Maus S., Barckhausen U., Berkenbosch H., et al. EMAG2: A 2–arc min resolution Earth Magnetic Anomaly Grid compiled from satellite, airborne, and marine magnetic measurements // Geochemistry, Geophysics, Geosystems. 2009. Vol. 10, no. 8. DOI: 10.1029/2009gc002471.
- *Meyer B., Saltus R., Chulliat A.* EMAG2v3: Earth Magnetic Anomaly Grid (2-arc-minute resolution) / NOAA National Centers for Environmental Information. 2017. DOI: 10.7289/V5H70CVX.
- *Petit C., Fournier M.* Present-day velocity and stress fields of the Amurian Plate from thin-shell finite-element modelling: Modelling Amurian Plate tectonics // Geophysical Journal International. 2004. Vol. 160, no. 1. P. 358–370. DOI: 10.1111/j.1365-246x.2004.02486.x.
- Sakhno V. G. Most recent and present-day volcanism of the southern Far East. Vladivostok: Dalnauka, 2008. 128 p. (In Russian).
- Tanaka A., Okubo Y., Matsubayashi O. Curie point depth based on spectrum analysis of the magnetic anomaly data in East and Southeast Asia // Tectonophysics. 1999. Vol. 306, no. 3/4. P. 461–470. DOI: 10.1016/s0040-1951(99)00072-4.
- *Wang J., Li C.-F.* Curie point depths in Northeast China and their geothermal implications for the Songliao Basin // Journal of Asian Earth Sciences. 2018. Vol. 163. P. 177–193. DOI: 10.1016/j.jseaes.2018.05.026.
- *Xiong S.-Q., Yang H., Ding Y.-Y., et al.* Characteristics of Chinese continent Curie point isotherm // Chinese Journal of Geophysics. 2016. Vol. 59, no. 6. P. 643–657. DOI: 10.6038/cjg20161008.
- Yarmolyuk V. V., Kozlovsky A. M., Travin A. V., et al. Duration and Geodynamic Nature of Giant Central Asian Batholiths: Geological and Geochronological Studies of the Khangai Batholith // Stratigraphy and Geological Correlation. 2019. Vol. 27, no. 1. P. 73–94. DOI: 10.1134/s0869593819010088.
- Zonenshain L. P., Savostin L. A. Introduction to Geodynamics. Moscow: Nedra, 1979. 311 p. (In Russian).